RSC Advances

ROYAL SOCIETY OF CHEMISTRY

www.rsc.org/advances

RSC Advances

RSCPublishing

ARTICLE

Metabolomics study on the cytotoxicity of graphene†

Cite this: DOI: 10.1039/x0xx00000x

Guozheng Jiao[a], Xin Li[*ab], Ning Zhang[c], Junqiang Qiu[c],Hongying Xu[c] and Shumin Liu[*c]

Received 00th January 2012,
Accepted 00th January 2012

DOI: 10.1039/x0xx00000x

www.rsc.org/

Gaphene has attracted enormous attention due to its unique and novel properties, showing great potential in different fields including biomedical engineering, tissue engineering, and biosensor. Thus, systematic investigation on the cytotoxicity of graphene is crucial to the further clinical use. However, there have been numerous contradictory reported results about the biocompatibility and cytotoxicity of graphene based on conventional in vitro toxicity test methods. We herein report a metabolomics approach to investigate the metabolic responses on graphene treated HepG2. Multivariate data analytic approaches reflected the significant difference in metabolic profiles between graphene-treated groups and control group. According to the results of analysis of variance (ANOVA), twelve metabolites had been detected as potential biomarkers. Moreover, three KEGG pathways including arginine and proline metabolism, purine metabolism, and glycophospholipid metabolism were identified. Our findings demonstrated that metabolomics would be an efficient platform to understand the molecular mechanism of cytotoxicity of graphene.

Introduction

Over the past decade, graphene has attracted increasing interest as drug delivery vehicle because of its unique physical, chemical, and other properties.[1,2] Despite advances in graphene-based drug delivery systems, challenges remain for carbon nanomaterials to clinical use. One of such challenges is exploring potential cytotoxic effects of carbon nanomaterials.[3] Safety is the first prerequisite for any nanomaterials used in biomedicine. *In vitro* toxicology testing provides an essential assessment of cell survival ability in the presence of nanomaterials,[4] which also can help to replace, reduce , and refine of animal experiments. Very recently, we and several other groups have devoted efforts to investigate the cytotoxicity of graphene as drug carriers or imaging probes.[5-15]

Many *in vitro* cytotoxicity assays have been described over the past few decades. Of these assays, 3-(4, 5-dimethylthiazol-2-yl)-2,5-diphenyltetrazolium bromide (MTT) assay is the most common *in vitro* nanotoxicity assessment. It relies on the cellular reduction of tetrazolium salts to form colored and insoluble formazan crystals.[16] Based on the same principle as MTT assay, water soluble tetrazolium salts (WST-1, WST-8) assays are also widely used to determine cell viability. This tetrazolium-based assay appeared to be a simple, rapid, cost-efficient, and reproducible sensitive test.[17] However, some studies on carbon nanomaterials obtained different cytotoxic results, and the conclusions of these studies varied dramatically. In a pilot study, Wörle-Knirsch *et al*. found that the interaction of single-walled carbon nanotubes with the MTT-formazan crystals caused misleading results of reduced cell viability.[18] Moreover, one study reported that the various dyes, such as commassie blue, alamar blue, neutral red, MTT, and WST-1 were not appropriate for the assessment of carbon nanotubes cytotoxicity.[19] Recent work by Liao *et al*. has shown that the MTT assay failed to predict the cytotoxicity of graphene-related materials.[20] Very recently, Chng and Pumera reported a conflicting testing result about the toxicity of graphene oxides by using two assays, the MTT assay and the WST-8.[21] It is important to note that traditional *in vitro* test methods have already been proven to be availableness for small molecule drug and chemical cytotoxicity. In comparison to chemicals, nanomaterials possess peculiar structural features and unique physicochemical properties. In general, the characteristics of nanomaterials such as size distribution, shape, surface property, and solubility, *etc*., are expected to play an important role in the accurate assessment of cellular activities. For example, anatase TiO_2 was found to be 100 times more cytotoxic than rutile TiO_2.[22] Furthermore, nanomaterials may interfere directly assay components, including dye molecules or enzymes, resulting in inaccurate data.[23, 24] Additionally, absorption and scattering of light by nanomaterials can also led to spurious results.[25] Consequently, even when using current *in vitro* cytotoxicity assays, unique properties of nanomaterials may represent major interferences for cytotoxicity assessments.[26] For graphene, it has been reported that graphene materials could induce interferences with *in vitro* assays through both optical and adsorptive effects.[27] Clearly, it is necessary to develop new approaches for full understanding of the *in vivo* toxicology before clinical applications of nanomaterials.

RSC Advances RSCPublishing

ARTICLE

Currently, "omics" technologies, such as genomics, proteomics and metabolomics, have been much appreciated for providing the quantitative, universal, integrated and predictive understandings of fundamental biological processes and biological systems.[28] Among of them, metabolomics (or metabonomics), specifically, is considered a robust tool that allows identification and quantitation of global small molecular mass metabolites (MW < 1kDa) in a given biological sample.[29, 30] The aim of metabolomics is to evaluate "the dynamic multi-parametric metabolic response of living systems to pathophysiological stimuli or genetic modification''.[31] Metabolomics is a high-throughput screening technique, and its data sets are generated mainly by two modern analytical platforms of nuclear magnetic resonance (NMR) spectroscopy and mass spectrometry (MS). With chemometrics tools, information provided by metabolomics studies may help in detailed and comprehensive understanding of the cytotoxic effects of nanomaterials.

In this work, a metabolomics technique based on ultra-high performance liquid chromatography (UPLC) coupled with quadrupole time-of-flight-mass spectrometry (Q-TOF-MS), combined with pattern recognition and metabolic pathway analysis, has been developed to investigate the metabolic responses on water-soluble graphene treated HepG2 cells. Twelve potential biomarkers and three related metabolic pathways were identified, which may offer new molecular mechanism information and in-depth understanding for the cytotoxicity of graphene.

Results and discussion

Characterization of water-soluble graphene

Water-soluble graphene nanosheets used in this case were prepared using our previously reported method.[14] The morphology and structure of the as-prepared graphene were characterized by scanning electron microscopy (SEM) and X-ray diffraction (XRD) analysis (Fig. 1). As can be seen in Fig. 1a, graphene has wrinkled surface and packed nanosheets. Fig. 1b shows a broad peak at around 2θ=26.3°, which is feature diffraction peak of graphene. It is clearly seen in Fig. 1c that our graphene can disperse well in aqueous solution and remain stable suspension over a long time. The above results confirm the successful preparation of water-soluble graphene.

Pattern recognition analysis of metabolic profiling

To comprehensively determine the endogenous metabolites effect of graphene on HepG2, the high efficient extraction strategy and the optimal UPLC-MS analytical conditions were performed to investigate the dose-dependent metabolic trajectory changes (ESI†). The base peak ion current chromatograms of samples in positive ionization mode were presented in Fig. S1 (ESI†). We pursued two multivariate data analytic approaches to differentiate metabolic changes of all

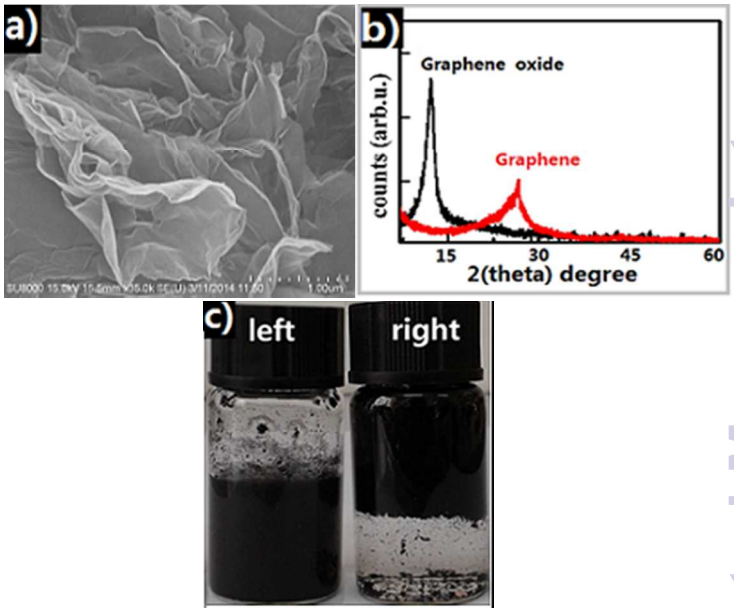

Fig. 1 SEM image of water-soluble graphene (a), XRD patterns of water-soluble graphene and graphene oxide (b), and the optical photographs of water-soluble graphene obtained (left) and control graphene (right) in aqueous dispersions (c).

samples and identify the potential biomarkers; an unsupervised approach based on principal components analysis (PCA) and a supervised approach based on partial least-squares-discriminant analysis (PLS-DA). In this work, PCA was firstly performed to classify the metabolic phenotypes. The PCA score plots of dose-dependent samples are presented in Fig.2a (24 h), Fig.S2a (48 h, ESI†), and Fig.S3a (72 h, ESI†), respectively.

In PCA score plot, a single data point represents a sample, and spots clustered together have more similar biochemical makeup than that of spots clustered apart.[32] The score plots demonstrate a sharp separation between the graphene-treated groups and control group at 24 h (Fig. 2a) and 72 h (Fig. S3a†) post-dose, suggesting that graphene did have a significant perturbation in the normal metabolic profiles of HepG2. However, the Low dose group was found to close to the control group at 48 h post-dose (Fig. S2a†), which indicate a slight separation between the control and low-dose groups. PLS-DA was then used to maximize the difference between groups. As shown in Fig. 2b, Fig. S2b†, and Fig.S3b†, the control groups could be clearly separated from the treated groups, and the treated groups were far away from each other, indicating the dose-dependent metabolic changes induced by graphene.

RSC Advances

RSCPublishing

ARTICLE

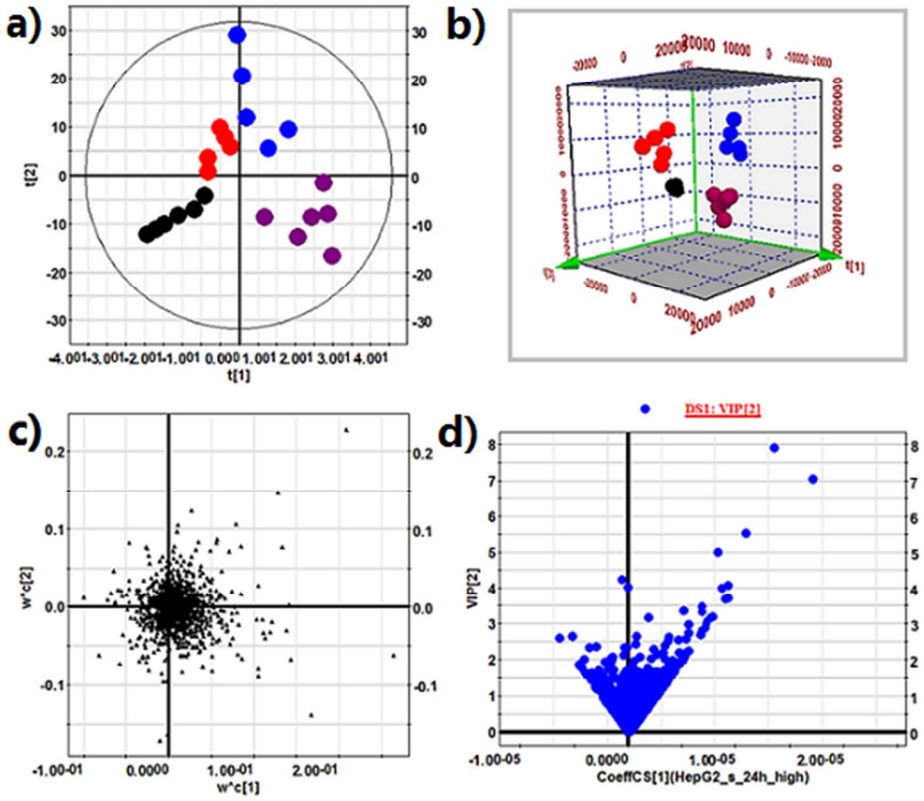

Fig. 2 Multivariate analysis of UPLC-Q-TOF-MS data for 24 h graphene-treated groups and control group. (a) PCA score plot. (b) 3D PLS-DA score plot. (c) Loading plot of PLS-DA. (d).VIP score plot from PLS-DA. Control group (black, graphene: 0 mg mL^{-1}), low dose group (red, graphene: 0.025 mg mL^{-1}), middle dose group (blue, graphene: 0.4 mg mL^{-1}), and high dose group (violet, graphene: 1 mg mL^{-1})

Additionally, trajectory analysis of score plots of PLS-DA showed significant biochemical perturbation for HepG2 induced by graphene even in the low-dose group. It should be noted that the low-dose level of graphene (0.025 mg/mL) in our study is lower than that of most previously reported graphene-based nanomaterials used as drug delivery and biodevices.

Identification of biomarkers

The use of loading and "variable importance in the projection" VIP-score plot in combination can detect differentiating metabolites and potential biomarkers. The loading plots (Fig. 2c, Fig.S2c†, and Fig.S3c†) and VIP plots (Fig. 2d, Fig.S2d†, and Fig.S3d†) generated after PLS-DA processing were applied to interpret the metabolic pattern, and visual show the weight of mass spectral signals attributed to the clustering and discrimination observed in the scores plot. Furthermore, a threshold of VIP values was set to 1.0. Using this protocol, 310 (24 h), 309 (48 h), and 307 (72 h) features were identified for further study.

A univariate analysis method, analysis of variance (ANOVA), was further performed to assess statistical validity of multivariate analysis and select potential biomarkers. The value (p<0.05) was set to statistical significance for graphene-treated group comparison with control group. In box and whisker plot (Fig.3), the signal intensities of 4 compounds were observed consistent decreases along the dose course. In contrast, the consistent increases in signal intensities of 8 metabolites were observed. As a result of univariate analysis, a total of 12 metabolites were detected and assumed as potential biomarkers.

Based on these potential biomarkers, heat-map, as a visual and quantitative evaluation approach, was constructed to further identify discriminatory metabolites by comparing the color patterns. The heat-map is presented in Fig. 4. Note, the color

RSC Advances RSCPublishing

ARTICLE

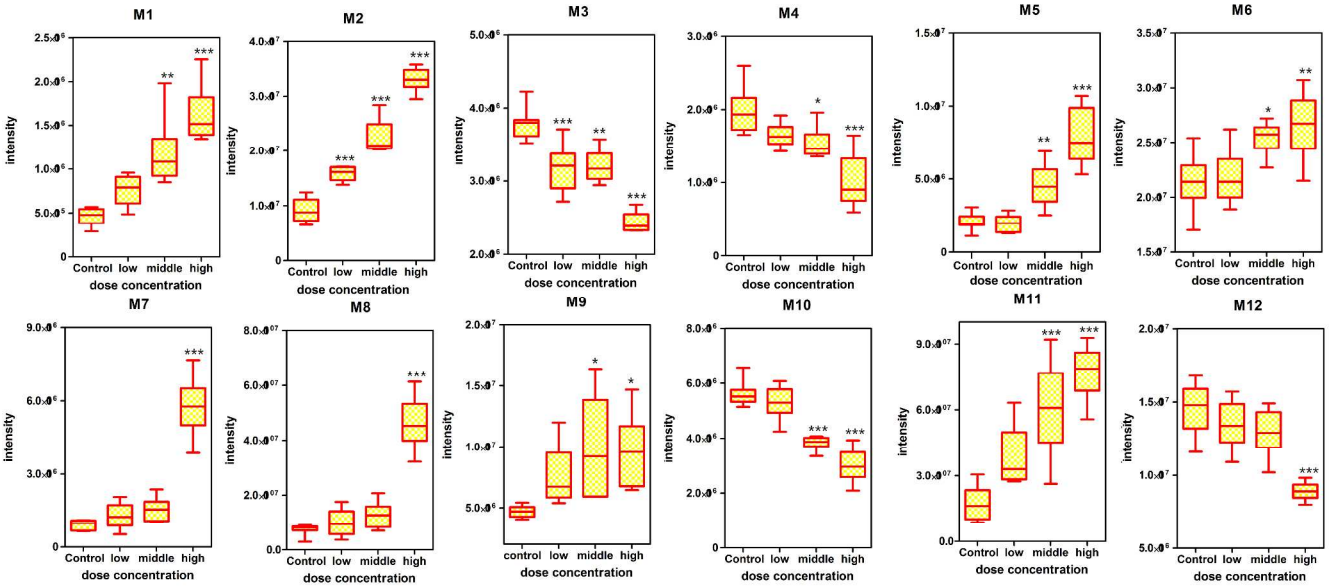

Fig. 3 ANOVA and box and whisker plot: Treated groups (low, middle, and high dose) compared to control groups. Statistical significance stands as "*" ($p < 0.05$), "**" ($p < 0.01$), and "***" ($p < 0.0001$).

scale bar on the left indicates the variety of metabolite content, and red rectangles represent a significant increase, on the contrary, green rectangles represent a significant decrease.[33] From color patterns comparison, eight samples exhibited an increasing trend from control groups to high groups, whereas four samples exhibited a decreasing trend. The heat-map further showed that the important differential metabolites as potential biomarkers.

Free databases of METLIN (http: //metlin.scripps.edu/), KEGG (http: //www. genome.jp/kegg/), HMDB (http: //www. hmdb. ca/), and MassBank (http://www.massbank.jp/) were used to confirm the possible chemical structures of potential biomarkers (Table 1). Among these metabolites, phospholipids and nitrogen-containing compounds were identified.

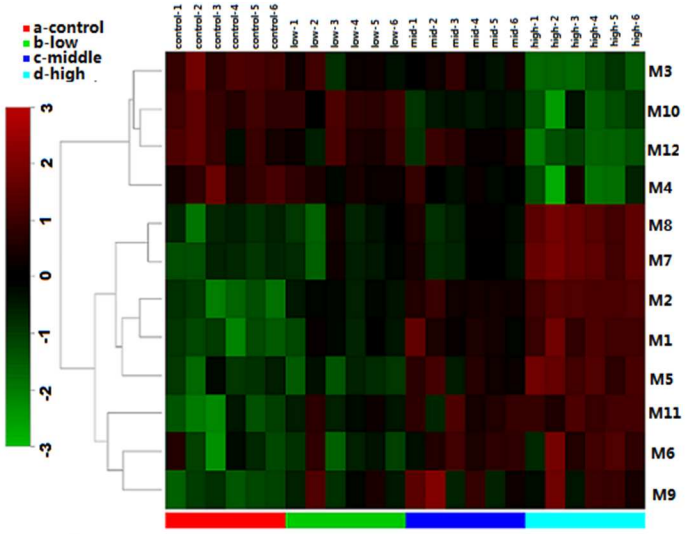

Fig. 4 Heat map visualization of identified marker metabolites. The color scale bar for heat intensity is shown top. The color bar indicates metabolite expression value, red rectangles represent a significant increase, and green rectangles represent a significant decrease. Rows: samples, columns: metabolites.

Metabolic pathway analysis

In order to further study the metabolic perturbation, analysis of metabolic pathways and networks influenced by graphene exposure was performed by using the KEGG database. The KEGG is an integrated database, and its pathway maps can provide biological interpretation of high-throughput data.[34] One of the main metabolic pathways, arginine and proline metabolism, was described in Fig. S4. As shown in Fig. S4, two potential biomarkers were found to be

Table1. Identification ofpotential biomarkers

Code	Rt	[M+R]+	Data	Formula	Name
M1	.1.76	[M+H]+	298.1285	$C_{14}H_{19}NO_6$	Phenethylamine glucuronide
M2	1.86	[M+NH_4]+	188.0778	$C_5H_6N_4O_3$	5-Ureido-4-imidazole carboxylatep
M3	8.12	[M+H]+	654.3264	$C_{37}H_{43}N5O6$	Unknown
M4	0.68	[M+H]+	132.0768	$C_4H_9N_3O_2$	Creatine
M5	1.25	[M+H]+	268.1040	$C_{10}H_{13}N_5O_4$	Adenosine
M6	6.49	[M+H]+	496.3398	$C_{24}H_50NO_7P$	1-Palmitoylglycerophosphocholine
M7	7.23	[M+Na]+	269.1220	$C_9H_{18}N_4O_4$	N_2-(D-1-Carboxyethyl)-arginine
M8	7.76	[M+H]+	256.2635	$C_{16}H_{33}NO$	Palmitic amide
M9	5.24	[M+H]+	281.1357	$C_{19}H_{13}N_5O_3$	Dihydrobiopterin
M10	6.22	[M+Na]+	494.3241	$C_{29}H_{45}NO_4$	Cervonyl carnitine
M11	7.91	[M+H]+	282.2791	$C_{18}H_{35}NO$	Oleamide
M12	6.66	[M+H]+	480.3449	$C_{24}H_50NO_6P$	LysoPC(18:1(9Z))

involved in the relevant pathway. A significant decrease in creatine (Cr) was observed from low-dose group to high-dose group. Cr is a nitrogenous organic compound and amino acid derivative synthesized from the arginine, glycine and methionine.[35] Cr, as an intracellular energy intermediate, plays a key role in safeguarding cellular energy storage and transmission.[36] Cr is also an antioxidant[37] and neurological nutrient.[38] The Cr metabolism disorder may lead to severe diseases. In contrast, the level of graphene was positive associated with N2-(D-1-Carboxyethyl)-arginine metabolite. Arginine is one of the most common amino acids, and it is helpful in synthesis of protein, nitric oxide, and urea.[39] From the pathway represented in Fig.S4, arginine was found to be involved in urea cycle. Urea cycle is an important metabolic pathway in which toxic ammonia produced from amino acid metabolism is converted into urea.[40] Graphene exposure may induce perturbations in urea cycle by changing the arginine concentrations. Besides the arginine and proline metabolism, two KEGG pathways, purine metabolism and glycophospholipid metabolism were also identified in the current study (Fig. S5† and Fig.S6†).

In the present investigation, significant perturbations of metabolite profiles had been found in graphene treated HepG2. Two possible cytotoxicity mechanisms of graphene could be suggested. One possibility is that graphene might cause physical damage in the cell membrane through direct interactions between graphene and cells, causing cytotoxicity to the cells.[41] The glycophospholipid metabolism in graphene treated cells as mentioned above could support this mechanism. Another possibility is that graphene might cause unfolding or false-folding protein accumulation, resulting in increasing energy requirements for protein synthesis,[42] which was consistent with the above discussed results of arginine and proline metabolism. Obviously, further work based on gene expression and proteomics levels is needed to focus on a more in-depth understanding of cytotoxicity of graphene.

Conclusions

In summary, we successfully demonstrated the effectiveness of applying metabolomics approach to investigate the cellular response to graphene. Twelve metabolites had been detected as potential biomarkers. Three pathways including arginine and proline metabolism, purine metabolism, and glycophospholipid metabolism can underlie the cytotoxicity of graphene. In addition, our findings not only indicated that exposure to graphene induced significant changes of metabolites in HepG2, but also provide a promising method for the understanding of cytotoxicity of graphene. It can be expected that metabolomics will be of great importance for evaluating biocompatibility of graphene-based materials.

Acknowledgements

We are grateful for the financial support from the National Natural Science Foundation of China (No. 21176052), the State Key Laboratory of Urban Water Resource and Environment, Harbin Institute of Technology (2013TS05), and Program for Innovation Research of Science in Harbin Institute of Technology.

Electronic Supplementary Information (ESI) available: additional experimental section, figure of the UPLC-MS BPI chromatography, multivariate analysis of UPLC-Q-TOF-MS data for 48h and 72h graphene-treated groups and control group, the trending figure of 12 univariate analysis, and pathway Fig..

Notes and references

[a] Department of Chemistry, Harbin Institute of Technology, Harbin 150090, China.
[b] State Key Lab of Urban Water Resource and Environment, Harbin Institute of Technology, Harbin 150090, China.
[c] Institute of Traditional Chinese Medicine, Key Laboratory of Chinese Materia Medica, Ministry of Education, Heilongjiang University of Chinese Medicine, Harbin 150040, China.
*E-mail: lixin@hit.edu.cn and keji-liu@163.com

1. Z. Liu, J. T. Robinson, S. M. Tabakman, K. Yang and H. J. Dai, *Mater. Today*, 2011, **14**, 316-323.
2. K. Yang, L. Z. Feng, X. Z. Shi and Z. Liu, *Chem. Soc. Rev.*, 2013, **42**, 530-547.
3. Y. B. Zhang, S. F. Ali, E. Dervishi, Y. Xu, Z. R. Li, D. Casciano and A. S. Biris, *ACS Nano*, 2010, **4**, 3181-3186.
4. D. S. Kohane and R. Langer, *Chem. Sci.*, 2010, **1**, 441-446.
5. Y. Z. Pan, H. Q. Bao, N. G. Sahoo, T. F. Wu and L. Li, *Adv. Funct. Mater.*, 2011, **21**, 2754-2763.
6. K. P. Liu, J. J. Zhang, F. F. Cheng, T. T. Zheng, C. M. Wang and J. J. Zhu, *J. Mater. Chem.*, 2011, **21**, 12034-12040.
7. G. Gollavelli and Y. C. Ling, *Biomaterials*, 2012, **33**, 2532-2545.
8. X. T. Zheng and C. M. Li, *Mol. Pharmaceutics*, 2012, **9**, 615-621.
9. K. Yang, L. L. Hu, X. X. Ma, S. Q. Ye, L. Cheng, X. Z. Shi, C. H. Li, Y. G. Li and Z. Liu, *Adv. Mater.*, 2012, **24**, 1868-1872.
10. H. Q. Hu, J. H. Yu, Y. Y. Li, J. Zhao and H. Q. Dong, *J. Biomed. Mater. Res. A*, 2012, 100A, 141-148.
11. Y. Li, Y. Liu, Y. J. Fu, T. T. Wei, L. Le Guyader, G. Gao, R. S. Liu, Y. Z. Chang and C. Y. Chen, *Biomaterials*, 2012, **33**, 402-411.
12. C. M. Santos, J. Mangadlao, F. Ahmed, A. Leon, R. C. Advincula and D. F. Rodrigues, *Nanotechnology*, 2012, **23**, 395101.
13. M. Wojtoniszak, X. C. Chen, R. J. Kalenczuk, A. Wajda, J. Lapczuk, M. Kurzewski, M. Drozdzik, P. K. Chu and E. Borowiak-Palen, *Colloid. Surface. B*, 2012, **89**, 79-85.
14. X. J. Fan, G. Z. Jiao, W. Zhao, P. F. Jin and X. Li, *Nanoscale*, 2013, **5**, 1143-1152.
15. X. J. Fan, G. Z. Jiao, L. Gao, P. F. Jin and X. Li, *J. Mater. Chem. B*, 2013, **1**, 2658-2664.
16. T. Mosmann, *J. Immunol. Methods*, 1983, **65**, 55-63.
17. N. J. Marshall, C. J. Goodwin and S. J. Holt, *Growth Regul.*, 1995, **5**, 69-84.
18. J. M. Worle-Knirsch, K. Pulskamp and H. F. Krug, *NanoLett.*, 2006, **6**, 1261-1268.
19. A. Casey, E. Herzog, M. Davoren, F. M. Lyng, H. J. Byrne and G. Chambers, *Carbon*, 2007, **45**, 1425-1432.
20. K. H. Liao, Y. S. Lin, C. W. Macosko and C. L. Haynes, *ACS Appl. Mater. Interfaces*, 2011, **3**, 2607-2615.
21. E. L. K. Chng and M. Pumera, *Chem.-Eur. J.*, 2013, **19**, 8227-8235.
22. C. M. Sayes, R. Wahi, P. A. Kurian, Y. P. Liu, J. L. West, K. D. Ausman, D. B. Warheit and V. L. Colvin, *Toxicol. Sci.*, 2006, **92**, 174-185.
23. B. J. Marquis, S. A. Love, K. L. Braun and C. L. Haynes, *Analyst*, 2009, **134**, 425-439.
24. C. Hirsch, M. Roesslein, H. F. Krug and P. Wick, *Nanomedicine,* 2011, **6**, 837-847.
25. B. Kong, J. H. Seog, L. M. Graham and S. B. Lee, *Nanomedicine*, 2011, **6**, 929-941.
26. A. Kroll, M. H. Pillukat, D. Hahn and J. Schnekenburger, *Eur. J. Pharm. Biopharm.*, 2009, **72**, 370-377.
27. M. A. Creighton, J. R. Rangel-Mendez, J. X. Huang, A. B. Kane and R. H. Hurt, *Small*, 2013, **9**, 1921-1927.
28. H. R. Tang and Y. L. Wang, *Prog. Biochem. Biophys.*, 2006, **33**, 401-417.
29. W. Weckwerth and O. Fiehn, *Curr. Opin. Biotechnol.*, 2002, **13**, 156-160.
30. J. K. Nicholson and J. C. Lindon, *Nature*, 2008, **455**, 1054-1056.
31. J. K. Nicholson, J. C. Lindon and E. Holmes, *Xenobiotica*, 1999, **29**, 1181-1189.
32. D. G. Robertson, *Toxicol. Sci.*, 2005, **85**, 809-822.
33. D. Toubiana, Y. Semel, T. Tohge, R. Beleggia, L. Cattivelli, L. Rosental, Z. Nikoloski, D. Zamir, A. R. Fernie and A. Fait, *PLoS Genet.*, 2012, **8**. e1002612.
34. M. Kanehisa, S. Goto, Y. Sato, M. Kawashima, M. Furumichi and M. Tanabe, *Nucleic Acids Res.*, 2014, **42**, D199-D205.
35. R. H. Andres, A. D. Ducraya, U. Schlattner, T. Wallimann and H. R. Widmer, *Brain Res. Bull.*, 2008, **76**, 329-343.
36. N. M. Verhoeven, G. S. Salomons and C. Jakobs, *Clin. Chim. Acta*, 2005, **361**, 1-9.
37. J. M. Lawler, W. S. Barnes, G. Y. Wu, W. Song and S. Demaree, *Biochem. Biophys. Res. Commun.*, 2002, **290**, 47-52.
38. E. Beard and O. Braissant, *J. Neurochem.*, 2010, **115**, 297-313.
39. S. M. Morris, *J. Nutr.*, 2007, **137**, 1602s-1609s.
40. J. Petrak, D. Myslivcova, P. Man, R. Cmejla, J. Cmejlova, D. Vyoral, M. Elleder and C. D. Vulpe, *Am. J. Physiol.-Gastroint. Liver Physiol.*, 2007, **292**, G1490-G1498.
41. W. B. Hu, C. Peng, M. Lv, X. M. Li, Y. J. Zhang, N. Chen, C. H. Fan and Q. Huang, *ACS Nano*, 2011, **5**, 3693-3700.
42. J. F. Yuan, H. C. Gao and C. B. Ching, *Toxicol. Lett.*, 2011, **207**, 213-221.

New insights into the cytotoxicity of graphene: Metabolomics analysis

Guozheng Jiao, Xin Li[b], Ning Zhang, Junqiang Qiu, Hongying Xu and Shumin Liu[*c]